Available online at www.eccomasproceedia.org
Eccomas Proceedia COMPDYN (2023) 2271-2285

ECCOMAS
Proceedia

COMPDYN 2023
9th ECCOMAS Thematic Conference on
Computational Methods in Structural Dynamics and Earthquake Engineering
M. Papadrakakis, M. Fragiadakis (eds.)
Athens, Greece, 12-14 June 2023

LOSS-BASED SEISMIC PRIORITISATION OF EXISTING RC GIRDER BRIDGES

Andrea Nettis[1], **Giuseppina Uva**[1]

[1]Department of Civil, Environmental, Land, Building Engineering and Chemistry
Polytechnic University of Bari, Bari, Italy
e-mail: {a.nettis, g.uva}@poliba.it

Abstract

In earthquake-prone countries, transport network managers need to perform extensive seismic risk prioritisation coping with a remarkable number of bridges characterised by a lack of knowledge data. This study proposes an efficient framework for risk-based prioritisation of bridges based on direct economic loss calculation including explicit consideration of knowledge-based uncertainty. The framework requires data on bridge structural and geometric features which can be collected based on existing blueprints or a fast on-site survey. Epistemic uncertainties are propagated by using statistical sampling techniques. It adopts a simplified analysis approach to perform fragility analysis and calculate losses in terms of the repair cost. The case-study section demonstrates the framework for eight simply supported girder bridges characterised by reinforced concrete single-column piers. The results in terms of fragility curves, loss ratio curves and expected annual losses are reported and discussed. Based on the results, it is possible to address more refined data collection and retrofit on critical bridges.

Keywords: seismic losses, bridges, risk assessment, risk prioritisation.

ISSN:2623-3347 Published by Eccomas Proceedia.
Peer-review under responsibility of the organizing committee of COMPDYN 2023.
doi: 10.7712/120123.10559.20998

1 INTRODUCTION

The structural performance of bridges under earthquake-induced excitations is crucial for maintaining the functionality and safety of transport networks in the emergency phase. However, in developed earthquake-prone countries, most of the bridges were designed in the past decades without appropriate anti-seismic criteria. Currently, considering large bridge portfolios, transport network authorities are responsible for addressing extensive seismic risk assessment plans for identifying bridges expected to have an inadequate response in seismic conditions and performing retrofit interventions. In this context, transport network operators need efficient approaches for performing such risk-based prioritisation and focus the available effort and resources on critical bridges enhancing the safety of entire networks. Taxonomy-based (i.e. typological) approaches can be adopted to identify critical bridges expected to exhibit an inadequate seismic response considering the hazard conditions of the location. These approaches assume that bridges belonging to the same typological class based on selected structural characteristics exhibit a similar seismic response. For example, parametric fragility curves for bridge typologies are reported in the well-known HAZUS technical manual. However, as evidenced by several studies [1, 2], typological approaches could neglect structure-specific characteristics which may be significant in determining the seismic response of a given bridge leading to inaccuracies in fragility estimations. According to Abarca et al. [2], typological approaches are accurate for achieving risk indicators related to entire portfolios and addressing funding by policymakers and insurance operators. However, a simplified structure-specific risk assessment should be preferred for retrofit prioritization purposes. Such simplified risk assessment requires efficient seismic performance and fragility analysis algorithms. These should involve a sustainable computational and modelling effort. Examples are provided by displacement-based bridge assessment algorithms [3–5] which rely on simplified equivalent elastic models and nonlinear static approaches leading to fragility estimations.

It is worth mentioning that the accuracy of risk-based prioritisation is significantly affected by the level of initial knowledge of the analysed bridges. Prioritisation plans should be based on preliminary knowledge of the analysed structures, based on easy-to-retrieve data, without resorting to accurate expensive surveys and diagnostic tests. Therefore, epistemic (knowledge-based) uncertainty, commonly related to e.g. unknown mechanical properties of materials, structural details or non-structural loads, should be considered when dealing with simplified seismic analysis oriented to risk prioritisation purposes.

Additionally, the effectiveness of a given risk prioritisation scheme strongly depends on the risk metric adopted to communicate risk to managers and stakeholders. The mean annual frequency of exceeding a given damage is often used to quantify the seismic risk by structural engineers. However, recent research developments support using losses such as repair cost, casualties, and loss-of-use duration, as risk metrics being easily understandable and transparent to decision-makers. The most advanced approach for loss assessment is proposed by the FEMA P-58 framework [6] and detailed for buildings where building losses are calculated based on the loss contribution of structural and non-structural components (so-called component-level approach). This latter requires significant computational efforts resulting hardly applicable within a risk prioritisation framework considering a relevant number of structures. Perdomo et al. [7] focus on the development of a component-level efficient displacement-based approach for economic loss assessment of continuous-deck bridges. Other simplified loss assessment approaches do not consider component-level contributions, but calculate economic losses based on a structure-level probability of damage. Several studies investigate procedures to calculate structure-level losses for bridges [8–10].

This study proposes an efficient framework for risk-based prioritisation of bridges based on direct loss calculation including explicit consideration of knowledge-based uncertainty. The framework requires data on bridge structural and geometric features which can be collected based on existing blueprints (if available) or a fast on-site survey. Epistemic uncertainties are propagated by using statistical sampling techniques. It adopts a simplified analysis approach to perform fragility analysis which, at this stage of development, can be applied for multi-span simply supported girder bridges. The risk is expressed by the expected annual losses considering the repair cost. To preliminary test the practical applicability, the framework is fully implemented in MATLAB environment through routines running provided that a source input spreadsheet is completed with essential deterministic and probabilistic knowledge data.

2 DESCRIPTION OF THE METHODOLOGY

The proposed framework to perform risk-based assessment of multi-span RC girder bridges considering easy-to-retrieve data is described in this section. The workflow is also shown in Figure 1. The different steps are presented in detail.

2.1 Data collection and modelling uncertainty

The framework requires initial knowledge data on the investigated bridge which should be collected by analysts in a tailored spreadsheet. The spreadsheet is composed of two parts. The first includes several sections aimed at collecting general data and geometric-structural parameters on the superstructure, substructure and girder-pier connection systems necessary for performing the calculations. As anticipated, the spreadsheet should be filled in by considering structural and geometric attributes which are collected through an onsite survey and available design blueprints. The list of input data, to be allocated in appropriate spreadsheet sections, is reported in Figure 1-step 1a and Table 1. The “general” section requires the determination of the structural scheme, distinguishing between simply supported (i.e. isostatic) and continuous (i.e. hyperstatic) superstructures. Additionally, the year of design is required, which is used to identify the reference design code. This latter, together with the traffic and seismic design category, is used for the simulated design. The sections “superstructure”, “substructure”, “abutments” and “bearings” are aimed at collecting knowledge data on the corresponding structural components. Unknown attributes related to the limited knowledge (e.g. material properties) are modelled via statistical distributions defined based on judgemental assumptions or available literature studies.

The second part of the spreadsheet (Figure 1-step 1b) is related to material mechanical properties and reinforcement details. In case of the unavailability of original blueprints, the routine can run a simulated design (Figure 1- step 1b) according to the design reference code and design material classes to assume realistic configurations of steel reinforcements in substructure components. In case the reinforcement details are known, these can be directly inserted into the spreadsheets and the simulated design is automatically deactivated.

For parameters which are unknown (blank cells in the input spreadsheet), the routine allows the user to assign statistical distributions as input. Those are defined with appropriate probability density functions and characteristic parameters (an example is provided in section 3) and can be judgementally assumed or retrieved from the literature. Examples of statistical distributions developed for bridge portfolios related to different geographical contexts are reported in Ref. [11–13].

Provided that the input is correct and complete, the framework foresees the simulation of knowledge-based uncertainties (Figure 1-step 2). Therefore, the random generation of a population of bridge model realisations is performed by means of statistical sampling

techniques. Particularly, the Latin Hypercube Sampling (LHS) [14] is used, which is more computationally efficient with respect to the standard Monte Carlo technique. After the statistical simulation is performed, N bridge model realisations are generated. Those exhibit the same deterministic variables, while different values are assigned to the parameters identified as epistemic uncertainty. For simplicity, no correlation among the random variables is considered, while full correlation of the random parameters within each bridge model realisation is assumed.

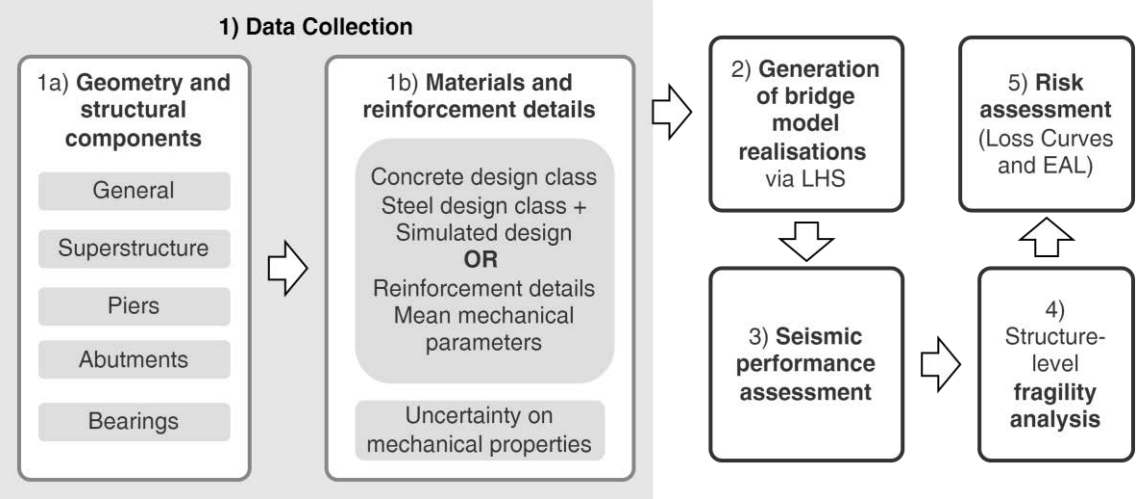

Figure 1. Overview of the framework.

General	Superstructure	Piers	Abutments	Bearings
- Structural scheme - Year of design - Traffic design category - Seismic design category	- Span length - Deck width - Walk board width - Girder height - Girder area - Number of girders - Slab thickness - Flexure moment of inertia (transverse dir.) - Non-struct loads	- Pier type - Pier dimensions - Pier height - Pier type - Pier cap height - Pier cap mass	- Deck-abut. gap - Backwall width - Backwall height	- Connection fixity (transv. dir.) - Connection fixity (long. dir.) - Bearing type - Bearing height - Distance between supports (long. dir.)

Table 1. Input data included in the spreadsheet.

2.2 Simplified modelling strategy

In the proposed framework, a simplified modelling and analysis strategy (Figure 1-step 3) is adopted to comply with the efficiency requirements which are desirable in dealing with the seismic assessment of portfolios of structures. The developed framework allows for analysing isostatic (simply supported girder bridges) and hyperstatic (continuous-superstructure) bridges. The analysis strategy assumes a nonlinear response for substructure components and girder-substructure connection systems, while an elastic response is assigned to the superstructure components. Soil-structure interaction is not considered.

Nonlinear static analysis concepts are used to calculate the seismic demand. First, an equivalent single-degree-of-freedom (SDoF) bilinear capacity curve (force-displacement relationship) is calculated for each superstructure-substructure subassembly. Each subassembly is composed of a substructure component (i.e. pier or abutment) and, if any, the components of the superstructure-substructure connection system (including bearing devices, shear keys, etc.).

Assuming the connection system and the pier (or abutment) acting as a series system under seismic excitations, the subassembly capacity curve is computed by combining the SDoF force-displacement relationships associated with both components. Approaches for calculating the force-displacement relationships are proposed in Ref. [3, 15] for piers, and in Ref. [16, 17] for other components. Additionally, an effective mass value is calculated for each subassembly as the sum of the tributary mass of the superstructure, of the pier cap and a third of the mass of the pier. Finally, for each subassembly, an equivalent viscous damping *vs* displacement ($\xi_{eq,sub} - \Delta_{sub}$) relationship is computed. To this aim, Equations (1) can be adopted to combine the equivalent viscous damping contributions by the substructure components ($\xi_{eq,p}$) and the girder-substructure connections system ($\xi_{eq,c}$) weighted by their corresponding displacement (Δ_p and Δ_c, respectively), . Particularly, the Equation (2) proposed by Priestley et al. [18] could be adopted to calculate the equivalent viscous damping for components characterised by a given hysteretic response. C_{evd} is a coefficient related to the type of hysteretic response which, for example, can be assumed equal to 0.444 for piers (Modified Takeda-thin hysteretic rule) and 0.565 for rubber bearings (elastic perfectly plastic hysteretic rule). The ξ_{eq} is based on the ductility demand μ for the investigated component and is calculated as the ratio between the displacement demand and the yielding displacement.

$$\xi_{eq,sub} = \frac{\Delta_p \xi_{eq,p} + \Delta_c \xi_{eq,c}}{\Delta_{sub}} \tag{1}$$

$$\xi_{eq} = 0.05 + C_{evd}\left(\mu - 1/\pi\mu\right) \tag{2}$$

The seismic response of a bridge realisation is modelled based on the subassemblies' capacity curves depending on the structural scheme. For continuous-superstructure bridges, the algorithm based on the displacement-based pseudo-pushover by Gentile et al. [3] can be efficiently adopted for achieving a bridge equivalent SDoF capacity curve (displacement Δ vs base shear V) related to the seismic action acting in transverse direction. This methodology consists of a series of progressive equivalent elastic analyses on a simple model represented by a single beam on inelastic supports simulating the bridge subassemblies. This algorithm directly allows for calculating a law relating the bridge equivalent viscous damping ξ_i for given Δ_i.

For the seismic action in the longitudinal direction, the equivalent SDoF capacity curve of the bridge is obtained by assuming the subassemblies act as a parallel system in resisting the total seismic inertia force. In this case, for a given equivalent SDoF displacement, each subassembly resists the total seismic inertia force depending on the proper effective stiffness. Therefore, the equivalent SDoF capacity curve can be computed, calculating the sum of the shear absorbed by the different subassemblies, assuming that these are subjected to the same top longitudinal displacement. In this case, the relationship between the bridge equivalent viscous damping ξ_i and a given Δ_i can be calculated via Equation (3).

$$\xi_i = \frac{\sum_{j=1}^{N} \xi_{eq,sub_j} V_{sub_j}}{\sum_{j=1}^{N} V_{sub_j}} \tag{3}$$

For multi-span simply supported girder bridges subjected to seismic action in the transverse direction, the individual pier model assumption can be applied [19]. According to this methodology, the bridge can be analysed assuming no transferring of seismic forces among the subassemblies responding as isostatic systems. In other words, each bridge subassembly is

analysed separately under a given seismic action and the damage of the weakest subassembly determines the damage of the bridge. This methodology assumes free relative rotations between adjacent independent superstructures and is accurate for first mode-dominated structures. According to Cardone [16], this condition is fulfilled if the ratio of the periods of adjacent independent subassemblies is contained within the range [0.5-2]. The individual pier model approach can be applied for the response in a longitudinal direction provided that the width of the expansion joint gap is sufficient to prevent interaction (or pounding) between adjacent superstructures. However, this method can not be applied if seismic retainers between the superstructure and substructure exist, or, for existing non-seismically designed bridges which usually exhibit low-width joints designed for thermal deformations only because of the premature closure of the gaps. In this case, the equivalent SDoF capacity curve of the bridge can be calculated under the above-mentioned parallel system assumption. It is worth mentioning that, if the closure of the deck-abutment joints is likely to happen, the nonlinear seismic response of the abutment-backfill subassembly should be considered when calculating the equivalent SDoF response of the bridge.

2.3 Seismic performance assessment

In the proposed framework, a probabilistic seismic performance assessment is carried out by including the uncertainty related to the record-to-record variability. To this aim, the Cloud-CSM proposed by the authors in a previous study [20] is applied. The use of the Cloud-CSM fosters the computational efficiency of this methodology with respect to other conventional approaches based on the use of nonlinear time history analysis (NLTHA), making the framework suitable for portfolio-scale assessment. According to the Cloud-CSM, the seismic demand for a given structure can be calculated based on the equivalent SDoF capacity curve and the response spectrum related to a given seismic excitation through a graphical approach carried out by using the acceleration-displacement plane. For each value of displacement Δ_i, the corresponding value of the secant period T_i is calculated. For each value of T_i, the overdamped seismic spectral demand is calculated by multiplying the elastic demand for an appropriate reduction coefficient η_i calculated via Equation (4). The seismic displacement demand for the structure subjected to a given seismic action is calculated as the abscissa corresponding to the graphical intersection between the capacity curve and the over-damped seismic demand.

$$\eta_i = \sqrt{0.07/(0.02 + \xi_i)} \tag{4}$$

2.4 Fragility analysis

The damage probability of a bridge for a given value of intensity measure (IM) is expressed by fragility curves. The approach adopted in this framework is aimed (Figure 1-step 4) to calculate the fragility curve related to each model realisation. Therefore, for a given case-study bridge, a fragility curve population is assigned. The variation in fragility among the model realisations informs the analyst on the influence of the epistemic uncertainty on bridge fragility. The approach for fragility analysis is explained as follows.

The seismic performance of a bridge model realisation under a given seismic excitation is categorised in damage states (DS) depending on appropriate displacement-based DS thresholds for the considered bridge components. A demand-capacity ratio (DCR) is used to evaluate the performance of each *i-th* component (e.g. pier, bearing, abutment) under the *j-th* ground motion, with respect to a given DS. The DCR is computed via Equation (5) where Δ_i^{DS} is the displacement-based DS threshold for the considered component. The maximum value of DCRs

computed for the bridge components is selected as bridge-level DCR and is used to synthetise the seismic performance of the bridge.

$$DCR_{ij}^{\mathrm{DS}} = \frac{\Delta_{ij}}{\Delta_i^{\mathrm{DS}}} \tag{5}$$

According to this approach for each bridge model realisation, a dataset of $[IM_j, DCR_j^{DS}]$ is calculated. A linear model relating the $[IM_j, DCR_j^{DS}]$ observations, transformed in the natural logarithmic scale, is fitted by using the least square regression method to obtain the relationship between the median DCR value conditioned to a given IM value ($\alpha_{DCR^{DS}|IM}$) as in Equation (6). The dispersion of DCR values around the median is computed ($\beta_{DCR^{DS}|IM}$) via Equation (7), where M is the number of ground motions, and assumed constant for each IM value.

$$\ln \alpha_{DCR^{DS}|IM} = \ln(a) + b \ln(IM) \tag{6}$$

$$\beta_{DCR^{DS}|IM} = \sqrt{\frac{\sum_{j=1}^{M} (\ln DCR_j^{DS} - \ln a(IM_j)^b)}{M-2}} \tag{7}$$

$$P(DS|IM) = P(DCR_{DS} > 1|IM) = 1 - \phi\left(\frac{-\ln \alpha_{DCR^{DS}|IM}}{\beta_{DCR^{DS}|IM}}\right) = \phi\left(\frac{\ln \alpha_{DCR^{DS}|IM}}{\beta_{DCR^{DS}|IM}}\right) \tag{8}$$

For each IM, the value of probability to reach a given DS, $P(DS|IM)$, corresponding to the probability of reaching a $DCR_{DS} > 1$ can be computed. Therefore, the fragility curve is represented by the normal cumulative distribution function $\phi(\cdot)$ in Equation (8).

This process is repeated for the entire dataset of bridge model realisations leading to a population of fragility curves expressing the influence of epistemic uncertainty on the bridge fragility. For a direct synthetic representation of the fragility curve population, appropriate fractiles of the probability to reach the DS for given values of IM are extracted. The 50th fractiles represent a synthetic bridge fragility curve including the uncertainty in terms of record-to-record variability and knowledge-based uncertainty. Moreover, the 16th and 84th fractiles (referred simply to as fragility fractiles hereafter), are adopted to identify a fragility "area" summarising the fragility variation depending on the knowledge-based uncertainty.

2.5 Risk and loss assessment

The fragility outcomes of the previous section are used for the risk assessment (Figure 1-step 5). In this study, the seismic risk is quantified by means of the total economic losses associated with the repairing of the damaged bridge. Only direct losses for bridge repairing are considered in this study, while no indirect losses (e.g. disruption time) are accounted for in seismic risk-based prioritisation. The process for calculating losses is based on the simplified structure-level approach implemented in the Hazus framework [21]. Note that other approaches, consisting of component-level loss calculation for bridges according to FEMA P-58 [6] are proposed in Ref. [10]. However, although more accurate, this latter requires larger computational effort and, therefore, is deemed not appropriate for seismic risk prioritisation scopes.

Consequence models, relating the loss ratio with respect to the mean replacement cost corresponding to each considered DS (i.e. damage-to-loss ratios, DLR) are needed in this process. These can be retrieved from the recommendations by Hazus [21] or developed by analysts with reference to the specific bridge. Provided that fragility curves are computed, the probability for a given structure of being in a given DS for a given IM value ($P_{DS_k}(IM)$) can

be calculated via Equation (9) in which N_{DS} is the number of considered DS thresholds. Loss curves $\mu_L(IM)$ relating the mean (expected) losses to IM values are calculated by multiplying the loss ratio curves $\mu_D(IM)$ calculated through Equation (10) for the total replacement cost (C_{REPL}).

$$P_{DS_k}(IM) = \begin{cases} P(DS_k|IM) - P(DS_{k+1}|IM), & k = 1, \dots, N_{DS} - 1 \\ P(DS_k|IM), & k = N_{DS} \end{cases} \quad (9)$$

$$\mu_D(IM) = \sum_{k=1}^{N_{DS}} DLR_k \, P_{DS_k}(IM) \quad (10)$$

Finally, the expected annual losses (EAL), which are used as a risk proxy in the proposed framework, can be computed by solving the integration between $\mu_L(IM)$ and the hazard curve related to investigated site $H(IM)$.

$$EAL = \int \mu_L(IM) \left| \frac{dH(IM)}{dIM} \right| dIM \quad (11)$$

Hazard curves $H(IM)$, representing the mean annual frequency of exceedance of a given seismic intensity for the site of interest, should be collected through a probabilistic hazard analysis for the bridge location.

In the proposed framework, this process is repeated for the fragility curves related to the selected fractiles of damage probability mentioned in subsection 2.4. Particularly, the EAL^{50th} is related to the 50th fragility fractile, while the EAL^{16th} and EAL^{84th}. EAL^{50th} can be directly used to perform seismic risk prioritisation reflecting the knowledge state for the considered bridges, while the amplitude of the interval between EAL^{16th} and EAL^{84th} is aimed to inform the analyst of the uncertainty around the EAL estimation and address further in-depth knowledge analysis where needed.

3 CASE-STUDY BRIDGE DATASET

3.1 Description of the case-study bridges

This section aims at demonstrating the application of the proposed framework for seismic risk-based prioritisation with reference to existing case-study bridges. Eight case-study RC girder bridges are identified within the Basilicata national road network in Southern Italy. These exhibit a variable number of spans, from two to seven, simply supported girder superstructures and single-column piers. General, geometric and structural characteristics of the case-study bridges are presented in Figure 2. Input knowledge data on the case studies are collected by means of fast onsite surveys aimed at filling the form described in subsection 2.1 which is necessary to run the risk assessment analyses. Since no design documents are available for the case studies and material tests are not carried out, the mechanical parameters of materials and reinforcement details are unknown. These are considered epistemic uncertainty and modelled by means of statistical distributions which are derived from previous studies [11, 13, 22]. These are reported in Table 2. Particularly, the design class of concrete and steel is modelled via uniform discrete distributions and a simulated design is performed within the framework to achieve a realistic value of reinforcements based on a given combination of concrete and steel design classes. For each design class, the f_{cm} and f_{ym} are derived and coefficients to obtain the f_c and f_y to be used within the calculations are randomly simulated. The bridges B1 to B7

exhibit non-seismically designed joint gaps between adjacent decks and between the decks and the abutments. Indeed, the joint gaps measure 20 to 25 mm for B1 to B7. For B8 the joint gap measures 70 mm.

Several assumptions are considered for the seismic response analyses. First, the individual pier model is applied for the analysis in the transverse direction neglecting the deformability and shear failure of fixed bearings. In the cases where shear keys are present, the nonlinear response of shear keys is neglected and a fixed girder-pier cap connection is assumed (since the girder-shear key gap size is reduced). Given the low gap width, the bridges are analysed as a parallel system in the longitudinal direction.

Parameter	Distribution	Parameters	
Characteristic (design) compressive strength of concrete (f_{ck})	Uniform (Discrete)	25-30-35	MPa
Characteristic (design) tensile strength of steel (f_{yk})	Uniform (Discrete)	375-440	MPa
Concrete compressive strength (f_c)	Normal	$\mu = 1$, $\sigma = 0.18$	Factor*
Steel tensile Strength (f_y)	Normal	$\mu = 1$, $\sigma = 0.09$	Factor*
Volumetric ratio of transverse reinforcements (ρ_t)	Uniform (Discrete)	~ 0.05-0.08	%
Shear modulus of neoprene bearings (G_{neo})	Uniform	l = 0.8, u = 1.2	MPa
Equivalent (passive) stiffness of the abutment backwall system (k_{abw})	Uniform	l = 11.5, u = 28.8	kN/mm/m
Non-structural gravity loads (W_{NS})	Uniform	l = 0.8, u = 1.2	Factor*

Table 2.Statistical distributions for knowledge-based uncertainty.

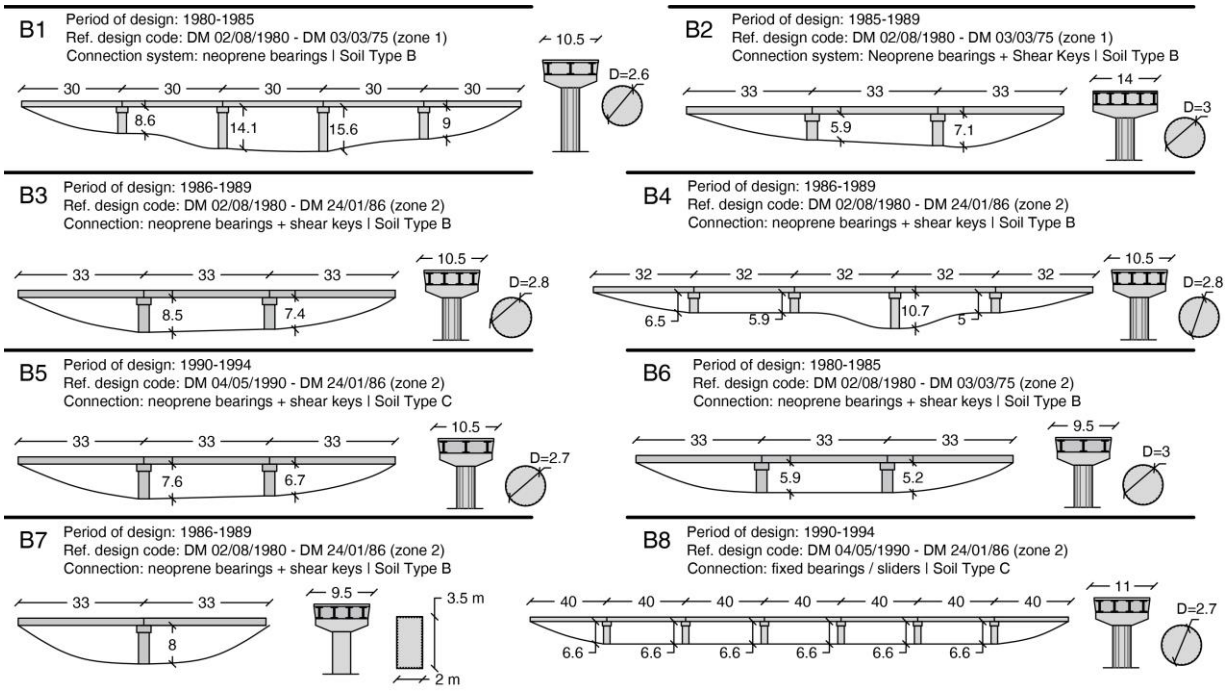

Figure 2. Geometric and structural characteristics of the case-study bridges.

3.2 Assumptions for the risk assessment

Assumptions in terms of seismic actions, seismic hazard analysis and DSs are described in this subsection.

The ground motion suite for modelling record-to-record variability in fragility analysis is composed of 100 natural ground motions selected from the SIMBAD database [23]. Based on this database, a first screening is performed to select records consistent with the characteristics of soil type, magnitude, and distance of expected earthquakes in the bridge locations. The magnitude and distance de-aggregation is achieved using the software REXEL [24]. After this first selection, the 100 records characterised by the highest peak ground acceleration are selected to perform the fragility analysis.

Seismic hazard curves representing the mean annual frequency for a given seismic intensity measure are selected. The probabilistic seismic hazard analysis is run by means of the REASSESS tool [25] by using the seismic source model by Meletti et al. [26]. For this purpose, the seismic intensity should be represented by appropriate IM parameters. In this case, the geometric average of the spectral accelerations ($AvgSa$) calculated within a significant range of period is chosen based on previous studies aimed to evaluate optimal IM by O'Reilly [27]. Two different IM parameters are used in the analysis, based on the seismic response in the longitudinal and transverse directions. In the former case, the $AvgSa$ is computed in a period interval between the bridge elastic (secant-to-yielding) first-mode period T_L and $1.5T_L$ (representing the period elongation). For the transverse response, the minimum value among the elastic periods of the subassemblies is extracted ($T_{T,min}$) and $AvgSa$ is computed in a period interval ranging between $T_{T,min}$ and $1.5T_{T,min}$. Particularly, two hazard curves related to the two adopted IMs are computed for each case-study bridge.

Five DS are used in this study. The displacement-based DS thresholds together with the DLRs associated with each DS are listed in Table 3. The DLRs are selected according to the Hazus methodology [21] and used by Padgett et al. [28]. The bridge mean replacement cost is calculated through the simplified approach by Zanini et al. [29], also applied, by Abarca et al. [2]. Clearly, appropriate calibrations of DLR and mean construction cost for the case studies analysed are desirable to improve the accuracy of the results of the framework.

Component	DS0	DS1	DS2	DS3	DS4
Piers (flexural)	0	Δ_y	$\Delta_y + 1/2(\Delta_u - \Delta_y)$	$\Delta_y + 2/3(\Delta_u - \Delta_y)$	Δ_u
Piers (shear)	0	-	-	Δ_{sh}	$1.1\ \Delta_{sh}$
Neoprene bearings	0	Δ_{fr}	$\Delta_{fr} + 1/2(\Delta_{pad} - \Delta_{fr})$	Δ_{pad}	Δ_{uns}
Abutment-backfill system	0	Δ_{gap}	$\Delta_{p,ab}$	$\Delta_{p,ab} + 2/3(\Delta_{u,ab} - \Delta_{p,ab})$	$\Delta_{u,ab}$
DLR	0	0.03	0.08	0.25	1

Pier - $\Delta_{y/u}$: yielding and ultimate displacement for flexure; Δ_{sh}: displacement corresponding to the shear failure.
Bearings - Δ_{fr}: the displacement corresponding to the friction strength attainment; Δ_{pad}: dimension of the pad; Δ_{uns}: displacement for girder unseating.
Abutment-backfill system - Δ_{gap}: the deck-abutment gap size; $\Delta_{p,ab}$: displacement at the reaching of passive backfill pressure; $\Delta_{u,ab}$: ultimate displacement of the back-wall

Table 3. Damage states thresholds and damage-to-loss ratios.

4 DISCUSSION OF RESULTS

4.1 Loss ratio curves

In this sub-section, results relevant to seismic risk-based prioritisation are shown and discussed. Figure 3 reports the loss ratio curves for the analysed case-study bridges. A synthetic loss curve for the given bridge including both record-to-record variability and epistemic uncertainty is represented as a continuous grey curve, while dotted curves express the variation range of loss ratios related to epistemic uncertainty only. Additionally, Figure 4 reports the fragility curves calculated for two selected bridge case studies for all the analysed DS. With reference to the response in the transverse direction (Figure 3a), a qualitative observation of the loss ratio fractiles reports that the largest uncertainty is related to B1, B5 and B8. The fragility curves in Figure 4a demonstrate that the large uncertainty in loss curves is clearly derived from the large uncertainty in terms of fragility. Considering the 50th loss ratio fractile, the most vulnerable bridges are B1, B2 and B3 reaching a 50% loss ratio for IMs equal to 0.90g, 0.93g and 0.89g, respectively.

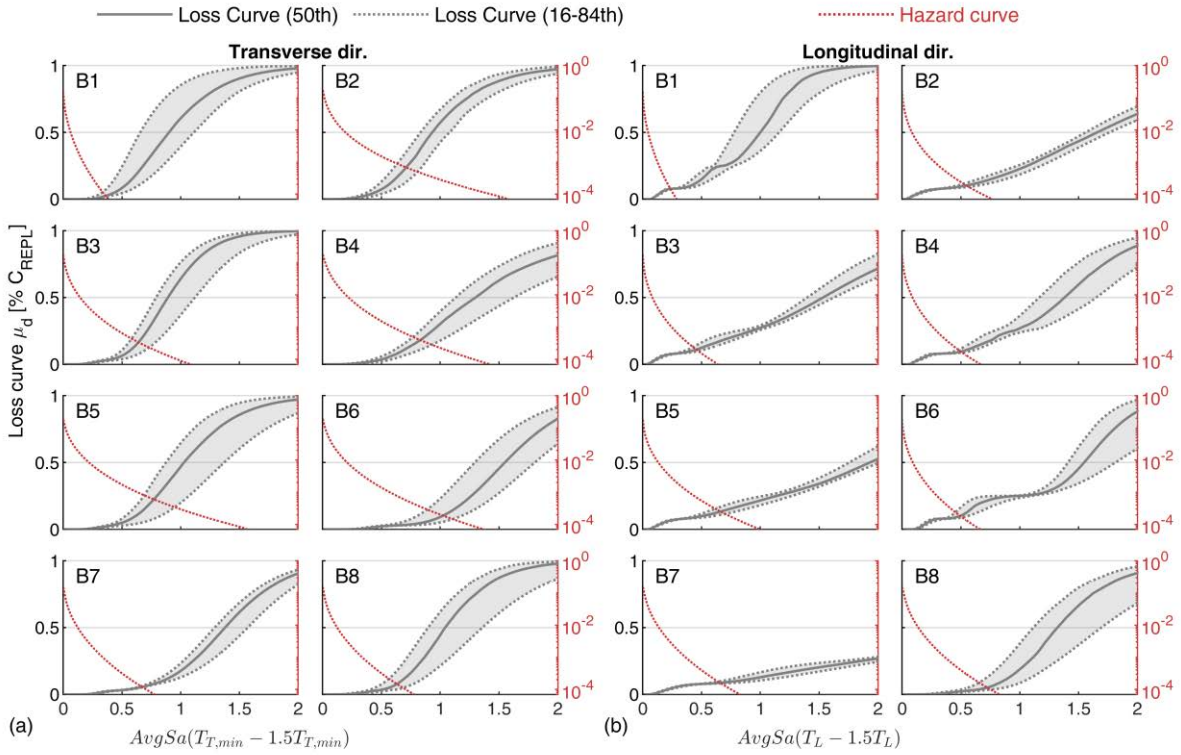

Figure 3. Loss ratio curves, expressing the losses in percentage of the total reconstruction cost, and hazard curves for the analysed case-study bridges: a) transverse direction; b) longitudinal direction.

For the seismic action in the longitudinal direction, Figure 3b shows that the cases B2, B3, B5 and B7 reach a 100% loss ratio for very large values of IMs, with negligible uncertainty, with respect to other cases such as B1 and B8. Figure 4c shows that, for B2, DS1 and DS2 are attained for very low values of IM. This effect is related to the gap closure between the deck and the abutments for weak IMs. Additionally, relevant uncertainty is associated with the transition between DS2 and DS3, while a negligible one is related to DS4. Considering that the most relevant loss contribution is associated with the DS4, this fragility result is reflected in the

low uncertainty on the loss ratio curves. A similar fragility pattern (not shown for brevity) is related to B3, B5 and B7.

A substantially different fragility pattern is related to bridge B8, Figure 4d shows that the DS1 is attained for higher IM values with respect to B2 (because of the larger deck-abutment gap size than other case-study bridges). In this case, a significant uncertainty is observed for the reaching of DS4 and, therefore, a large variability is achieved in terms of loss ratio curves.

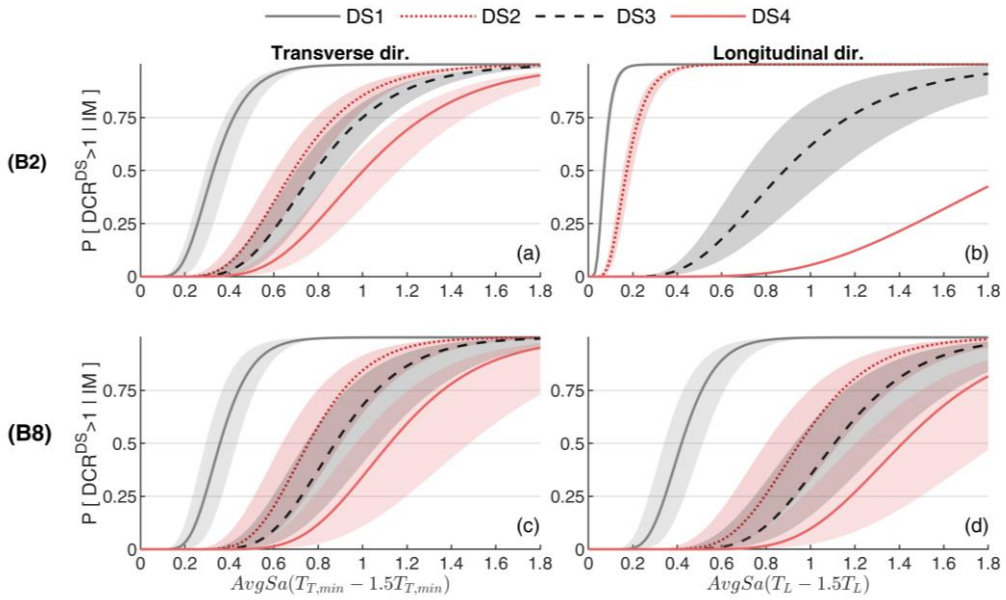

Figure 4. Fragility curves and corresponding uncertainty for two case-study bridges (a-b) B2; (c-d) B8.

4.2 Loss assessment

The loss ratio curves discussed in the previous subsection are combined together with the total replacement cost and the hazard curves to calculate EAL. Hazard curves computed for each of the case-study bridges are shown in Figure 3 as red dotted lines. EAL^{50th} are computed based on the 50th loss ratio fractiles and shown in Figure 5. EAL^{50th} includes the contribution of the cumulative uncertainty related to both the record-to-record variability and the knowledge-based uncertainty. In addition, EAL^{16th} and EAL^{84th} are also computed by using 16th and 84th loss ratio fractiles and shown as error bars in Figure 5. EAL^{50th} can be directly used for seismic risk prioritisation. B2 and B5 are associated with the highest value of EAL^{50th} and, therefore, should be considered the most critical bridges within the analysed group. A low uncertainty expressed by the range [EAL^{16th} - EAL^{84th}] is associated with the response in longitudinal direction. Conversely, the effect of knowledge-based uncertainty is large for B2 and B5 analysed in the transverse direction. Based on these results, appropriate in-depth data collection should be directed by transport managers' analysts to these cases. Another run of the framework can be easily carried out considering the availability of new refined knowledge data on e.g. constructive details, and mechanical properties. Based on a re-calculation of the EAL^{50th}, the analysts are in charge of addressing retrofit where needed.

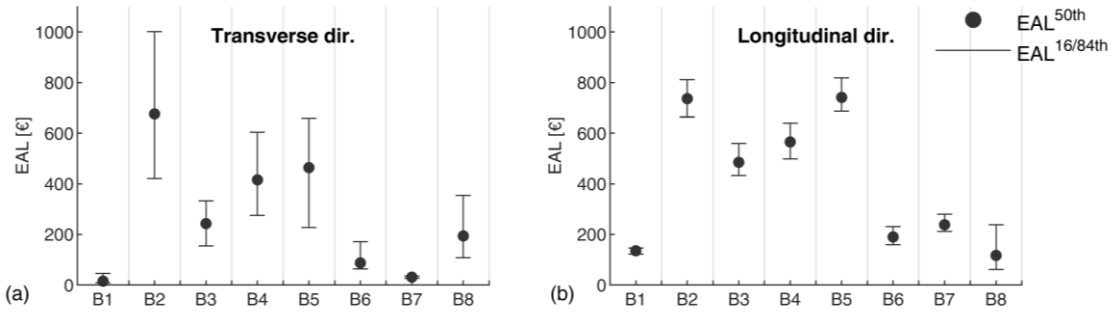

Figure 5. Expected annual losses for the analysed case studies: a) transverse direction; b) longitudinal direction.

5 CONCLUSION

An efficient framework for risk-based prioritisation of bridges based on direct loss calculation is presented in this study. It includes explicit consideration of knowledge-based uncertainty and can be used for addressing refined surveys and retrofit on portfolios composed of bridges characterised by a low level of knowledge. The framework requires data on bridge structural and geometric features which can be easily collected. The methodology is designed to be efficient and suitable for portfolio-level analyses, requiring a low computational and modelling effort. Clearly, the simplicity is reflected in a lower accuracy with respect to more refined analysis methods (e.g. nonlinear time history analyses and component-based loss assessment). These latter can be used for a more accurate risk assessment on the cases which are described as most critical based on the results of the proposed approach.

The presented framework is applied to a dataset of eight case-study simply supported girder bridges characterised by single-column piers. The methodology for considering knowledge-based uncertainty is described. The results in terms of fragility curves, loss ratio curves and expected annual losses are reported. Based on the results, it is possible to prioritise more refined data collection and retrofit on critical bridges. At this stage of development, only direct economic losses, in terms of repair cost, are considered. However, further advances should be aimed at including indirect losses which can be significant for risk prioritisation purposes.

ACKNOWLEDGEMENTS

The authors acknowledge the Italian Consortium FABRE for the financial support given to the research study through the 1-year research grant 2022-2023: "*Development and implementation of multi-level approaches for multi-hazard risk analysis and structural safety assessment of existing bridges and viaducts*". The second author acknowledges funding by Centro Nazionale Sustainable Mobility Center, within the framework of "MOST" project, CUP code: D93C22000410001.

REFERENCES

[1] S. P. Stefanidou, A. J. Kappos, Bridge-specific fragility analysis: when is it really necessary?, *Bulletin of Earthquake Engineering*, **17**, no. 4, 2245–2280, 2019, doi: 10.1007/s10518-018-00525-9.

[2] A. Abarca, R. Monteiro, G. J. O'Reilly, Exposure knowledge impact on regional seismic risk assessment of bridge portfolios, *Bulletin of Earthquake Engineering*, **20**, no. 13, 7137–7159, 2022, doi: 10.1007/s10518-022-01491-z.

[3] R. Gentile, A. Nettis, D. Raffaele, Effectiveness of the Displacement-Based seismic

performance Assessment for continuous RC bridges and proposed extensions, *Engineering Structures*, 2020, doi: 10.1016/j.engstruct.2020.110910.

[4] A. Nettis, P. Iacovazzo, D. Raffaele, G. Uva, J. M. Adam, Displacement-based seismic performance assessment of multi-span steel truss bridges, *Engineering Structures*, **254**, no. July 2021, 113832, 2022, doi: 10.1016/j.engstruct.2021.113832.

[5] M. Cademartori, T. J. Sullivan, S. Osmani, Displacement - based assessment of typical Italian RC bridges, *Bulletin of Earthquake Engineering*, no. 0123456789, 2020, doi: 10.1007/s10518-020-00861-9.

[6] Federal Emergency Management Agency (FEMA), Seismic Performance Assessment of Buildings, Volume 1 – Methodology, *Fema P-58-1*, **1**. Washington DC, 2012. [Online]. Available: www.ATCouncil.org

[7] C. Perdomo, R. Monteiro, Extension of displacement-based simplified procedures to the seismic loss assessment of multi-span RC bridges, *Earthquake Engineering and Structural Dynamics*, 2020, doi: 10.1002/eqe.3389.

[8] Y. Dong, D. M. Frangopol, Risk and resilience assessment of bridges under mainshock and aftershocks incorporating uncertainties, *Engineering Structures*, **83**, 198–208, 2015, doi: 10.1016/j.engstruct.2014.10.050.

[9] A. Miano, F. Jalayer, R. De Risi, A. Prota, G. Manfredi, Model updating and seismic loss assessment for a portfolio of bridges, *Bulletin of Earthquake Engineering*, **14**, no. 3, 699–719, 2016, doi: 10.1007/s10518-015-9850-y.

[10] C. Perdomo, A. Abarca, R. Monteiro, Estimation of Seismic Expected Annual Losses for Multi-Span Continuous RC Bridge Portfolios Using a Component-Level Approach, *Journal of Earthquake Engineering*, **26**, no. 6, 2985–3011, 2022, doi: 10.1080/13632469.2020.1781710.

[11] B. G. Nielson, R. DesRoches, Seismic fragility methodology for highway bridges using a component level approach, *Earthquake Engineering and Structural Dynamics*, 2007, doi: 10.1002/eqe.655.

[12] D. H. Tavares, J. E. Padgett, P. Paultre, Fragility curves of typical as-built highway bridges in eastern Canada, *Engineering Structures*, **40**, 107–118, 2012, doi: 10.1016/j.engstruct.2012.02.019.

[13] C. Zelaschi, R. Monteiro, R. Pinho, Parametric Characterization of RC Bridges for Seismic Assessment Purposes, *Structures*, **7**, 2016, doi: 10.1016/j.istruc.2016.04.003.

[14] A. Olsson, G. Sandberg, O. Dahlblom, On Latin hypercube sampling for structural reliability analysis, *Structural Safety*, 2003, doi: 10.1016/S0167-4730(02)00039-5.

[15] M. J. N. Priestley, G. M. Calvi, M. J. Kowalsky, Displacement-based seismic design of bridges, in *Bridge Engineering Handbook: Seismic Design, Second Edition*, 2014. doi: 10.1201/b15663.

[16] D. Cardone, Displacement limits and performance displacement profiles in support of direct displacement-based seismic assessment of bridges, *Earthquake Engineering and Structural Dynamics*, 2014, doi: 10.1002/eqe.2396.

[17] B. G. Nielson, Analytical fragility curves for highway bridges in moderate seismic zones, 2005. doi: 10.1016/j.engstruct.2017.03.041.

[18] M. J. N. Priestley, G. M. Calvi, M. J. Kowalsky, *Displacement-based seismic design of structures*. IUSS Press, Pavia, Italy, 2007.

[19] P. E. Pinto, P. Franchin, Issues in the upgrade of Italian highway structures, *Journal of Earthquake Engineering*, **14**, no. 8, 1221–1252, 2010, doi: 10.1080/13632461003649970.

[20] A. Nettis, R. Gentile, D. Raffaele, G. Uva, C. Galasso, Cloud Capacity Spectrum Method: accounting for record-to-record variability in fragility analysis using nonlinear static procedures, *Soil Dynamics and Earthquake Engineering*, 2021, doi: 10.1016/j.soildyn.2021.106829.

[21] Federal Emergency Management Agency (FEMA), Hazus Earthquake Model Technical Manual - Hazus 5.1. Federal Emergency Management Agency (FEMA), 2022. [Online]. Available: https://www.fema.gov/sites/default/files/documents/fema_hazus-earthquake-model-technical-manual-5-1.pdf

[22] P. Tortolini, M. Petrangeli, A. Lupoi, Criteri per la verifica e la sostituzione degli appoggi in neoprene di viadotti esistenti in zona sismica, in *14th italian conference on seismic engineering (ANIDIS)*, 2011, no. October 2014. [Online]. Available: https://www.researchgate.net/publication/266941512

[23] C. Smerzini, C. Galasso, I. Iervolino, R. Paolucci, Ground motion record selection based on broadband spectral compatibility, *Earthquake Spectra*, **30**, no. 4, 1427–1448, 2014, doi: 10.1193/052312EQS197M.

[24] I. Iervolino, C. Galasso, E. Cosenza, REXEL: Computer aided record selection for code-based seismic structural analysis, *Bulletin of Earthquake Engineering*, 2010, doi: 10.1007/s10518-009-9146-1.

[25] E. Chioccarelli, P. Cito, I. Iervolino, M. Giorgio, REASSESS V2.0: software for single- and multi-site probabilistic seismic hazard analysis, *Bulletin of Earthquake Engineering*, 2019, doi: 10.1007/s10518-018-00531-x.

[26] C. Meletti *et al.*, A seismic source zone model for the seismic hazard assessment of the Italian territory, *Tectonophysics*, 2008, doi: 10.1016/j.tecto.2008.01.003.

[27] G. J. O'Reilly, Seismic intensity measures for risk assessment of bridges, *Bulletin of Earthquake Engineering*, 2021, doi: 10.1007/s10518-021-01114-z.

[28] J. E. Padgett, R. Desroches, E. Nilsson, Regional seismic risk assessment of bridge network in Charleston, South Carolina, *Journal of Earthquake Engineering*, **14**, no. 6, 918–933, 2010, doi: 10.1080/13632460903447766.

[29] M. A. Zanini, C. Pellegrino, R. Morbin, C. Modena, Seismic vulnerability of bridges in transport networks subjected to environmental deterioration, *Bulletin of Earthquake Engineering*, **11**, no. 2, 561–579, 2013, doi: 10.1007/s10518-012-9400-9.